Chiral separation of substituted phenylalanine analogues using chiral palladium phosphine complexes with enantioselective liquid–liquid extraction†

Bastiaan J. V. Verkuijl,[a] Boelo Schuur,[b] Adriaan J. Minnaard,*[a] Johannes G. de Vries*[a,c] and Ben L. Feringa*[a]

Received 25th November 2009, Accepted 30th March 2010
First published as an Advance Article on the web 17th May 2010
DOI: 10.1039/b924749a

Chiral palladium phosphine complexes have been employed in the chiral separation of amino acids and phenylalanine analogues in particular. The use of (*S*)-xylyl-BINAP as a ligand for the palladium complex in enantioselective liquid–liquid extraction allowed the separation of the phenylalanine analogues with the highest operational selectivity reported to date. ^{31}P NMR, FTIR, FIR, UV-Vis, CD and Raman spectroscopy methods have been applied to gain insight into the binding mechanism of the amino acid substrates with the chiral palladium phosphine complexes. A complexation in a bidentate fashion is proposed.

Introduction

The preparation of enantiomerically pure compounds is a major contemporary challenge in the pharma and chemical industry.[1] The methods available to access enantiopure compounds include resolution of racemates, the chiral pool, fermentation, asymmetric catalysis and biocatalysis, with resolution being the major source.[2] The repetoir of currently available resolution methods comprises resolution *via* crystallisation of diastereomeric salts, *i.e.* classical resolution,[3] kinetic resolution[4] using enzymes or chiral catalysts, or dynamic kinetic resolution.[5] Sometimes the undesired enantiomer can be racemised and recycled.[6] Despite the theoretical maximum of 50% yield classic resolution is still a widely applied method in the fine chemical and pharmaceutical industries.[7] The labor intensiveness and the problems with reproducibility it suffers from, provides considerable incentives to find alternative solutions.[8] Currently among the methods being explored are resolution with *in situ* racemization,[9] membrane-assisted separations,[10] diastereomer separation by distillation,[11] supercritical extraction,[12–14] fractional enantioselective extraction [15,16] and chiral simulated moving bed (SMB).[17]

In enantioselective liquid–liquid extraction (ELLE), an enantiopure host is used as an extractant to bind enantiospecifically and reversibly with a racemic substrate (Fig. 1). If the host is confined to one phase in a biphasic system, an enantiomeric separation of the substrate can take place between the two phases in a single step. If the separation is imperfect, a fractional extraction series is required.[18,19] A minimal selectivity of 1.5 is generally perceived as necessary to achieve separation within a reasonable number of fractional extraction steps.[20] Important features of this approach are its potential versatility and ease of operation. It is possible to develop hosts which, for instance, separate the racemates of an entire class of compounds.

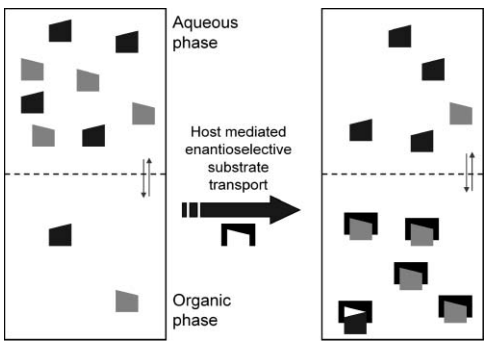

Fig. 1 Schematic representation of enantioselective liquid–liquid extraction. Symbols: grey blocks: (*S*)-substrate, black blocks: (*R*)-substrate, bold brackets: host.

Typically U-tubes or membranes are employed in separation schemes where the chiral host is applied in a catalytic fashion. The use of a number of membranes in series has even allowed for complete separation.[21] Maier, Lindner and co-workers have reported the use of a centrifugal partition chromatograph containing an MTBE solution of bis-1,4-(dihydroquinidinyl)phthalazine as the stationary chiral host solution which was able to fully separate the herbicide 2-(2,4-dichlorophenoxy)propionic acid (dichlorprop) which was fed as a solution in aqueous buffer as the mobile phase.[22] Since these methods suffer from problems regarding scalability, we have developed the use of centrifugal separators as a highly efficient method for continuous extraction.[23–25] Applying a number of these in series allows for the full separation of a racemate.[26]

A fractional extraction centrifugal contactor separator cascade (CCS cascade) is depicted in Fig. 2. The fractional extraction is based on the principle of countercurrent extraction, giving the optimal separation in as low a number of stages as possible and the optically pure substrate in the raffinate (1).[19] Every stage represents a centrifugal contactor separator (CCS) which is a table top apparatus capable of mixing and separating two liquid phases in a continuous fashion. The extraction of the host, which is defined as back extraction (Fig. 2, right) gives the other enantiomer of the

[a]*Laboratories for Organic Chemistry, Stratingh Institute for Chemistry, University of Groningen, Nijenborgh 4, 9747 AG, Groningen, The Netherlands*
[b]*Eindhoven University of Technology, Department of Chemistry and Chemical Engineering, Den Dolech 2, 5600 MB, Eindhoven, The Netherlands*
[c]*DSM Innovative Synthesis BV, P.O. Box 18, 6160, MD Geleen, The Netherlands*

† Electronic supplementary information (ESI) available: Experimental and analytical details. See DOI: 10.1039/b924749a

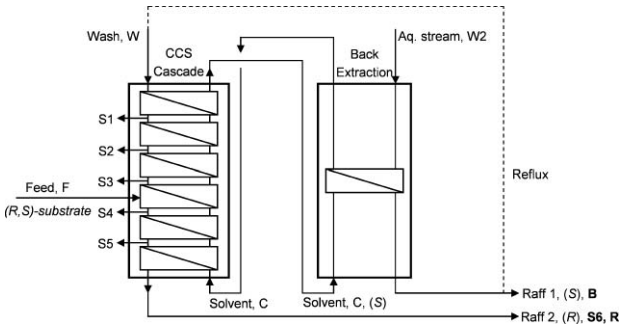

Fig. 2 Fractional extraction cascade scheme.

substrate in the raffinate (2). The host acts in a reversible manner and remains in a closed cycle. As a result, the separation of the substrate occurs as a continuous process.

The relationship between the minimal amount of required fractional extraction steps (N_{min}) for full separation of both enantiomers of the substrate, the desired ee of the substrate and the operational selectivity (α_{op}) of a single extraction, is described by the Fenske equation (eqn (1)).[27]

$$N_{\min} = \frac{\ln\left(\frac{x_R/(1-x_R)}{x_s/(1-x_s)}\right)}{\ln \alpha_{op}} \quad (1)$$

The relationship between N_{min} and α_{op} is shown in Fig. 3a. At an α_{op} of 1.5, N_{min} is still 25. N_{min} drops rapidly as α_{op} increases, leaving only 10 steps when $\alpha_{op} = 3.0$. N_{min} subsequently lowers more slowly and 5 extraction steps remain at $\alpha_{op} = 8.0$. It can be concluded, that full separation is already possible at moderate levels of α_{op} by using a fractional extraction CCS cascade with a reasonable number of fractional steps. A further increase in α_{op} provides only a minor decrease in N_{min}. The relationship between the desired ee and N_{min} is depicted in Fig. 3b. For an $\alpha_{op} = 7.0$, only 4 steps are required to obtain 95% ee. Higher ee is dependent on the number of extraction steps. To achieve 99% ee, 6 steps are required. An additional step provides 99.8% ee.

Over and above the technological aspects, the development of improved chiral host compounds is essential. In particular the enantioselective extraction of underivatized amino acids is one of the key challenges within the field of ELLE. The work of Cram *et al.* demonstrates that high selectivities could be achieved for a range of amino acid perchlorate salts using crown ethers with a functionalized BINOL backbone.[28;29] Subsequently, De Mendoza and co-workers combined a chiral guanidinium group with a crown-ether to extract tryptophan enantioselectively (Fig. 4).[30] Metal complexes as hosts have been employed including lanthanide β-diketonate[31] and copper-proline complexes.[20,32] Recently we have shown that the use of the metal complex $PdCl_2$((*S*)-BINAP) as a host results in the highest operational selectivity for underivatized tryptophan in an ELLE system using metal complexes reported to date.[33] This system meets all the necessary requirements regarding selectivity, control of distribution and reversibility for future application in a CCS cascade.

Here, we report the use of the (*S*)-xyl-BINAP ligand for the palladium host, which results in the highest selectivities for a range of phenylalanine derivatives reported to date and the highest selectivity for phenylalanine achieved in ELLE using metal

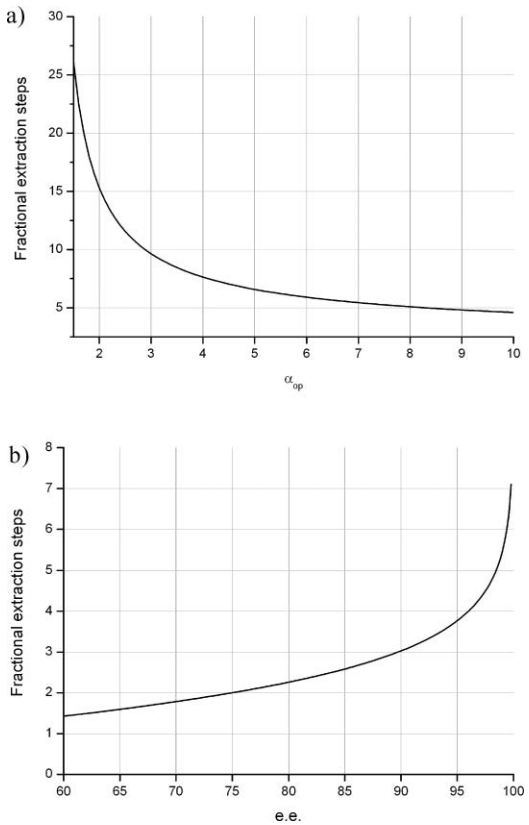

Fig. 3 Minimal number of fractional extraction steps needed (N_{min}) *versus* α_{op} where ee = 99% (a) and ee where $\alpha_{op} = 7.0$ (b).

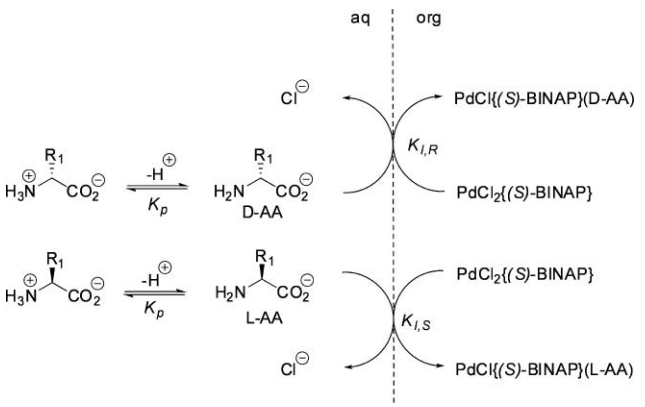

Fig. 4 General extraction scheme.

complexes as hosts. Furthermore, several spectroscopic methods are used to gain insight into the structure of the complex, which results in the structure presented in this article.

Results and discussion

Ligands

The effect of structural variation of the ligand which is complexed to the palladium-ion was explored using BINAP analogues. In addition, the extraction behavior of the palladium (*S*)-BINAP and (*R*)-BINAP complexes was tested. The complexes were formed *in situ* by stirring a solution of 1.1 eq. of ligand overnight with 1.0 eq. of the palladium precursor [$PdCl_2(CH_3CN)_2$] and the

Table 1 Ligand screening

Entry	Ligand	Substrate	[host]	D(org/aq)[a]	α_{op}[b]
1	(*R*)-BINAP	Trp	5.0	0.2	2.2
2	(*R*)-BINAP	Trp-Na[a]	5.0	2.0	2.3
3	(*R*)-BINAP	Trp	1.0	0.1	2.2
4	(*R*)-BINAP	Trp-Na	1.0	0.5	2.4
5	(*S*)-tol-BINAP	Trp	5.0	0.2	1.7
6	(*S*)-tol-BINAP	Trp-Na	5.0	2.6	1.5
7	(*S*)-tol-BINAP	Trp	1.0	0.1	1.8
8	(*S*)-tol-BINAP	Trp-Na	1.0	0.5	1.6
9	(*S*)-xylyl-BINAP	Trp	5.0	0.2	3.0
10	(*S*)-xylyl-BINAP	Trp-Na	5.0	2.9	3.1
11	(*S*)-xylyl-BINAP	Trp	1.0	0.1	3.1
12	(*S*)-xylyl-BINAP	Trp-Na	1.0	0.6	3.2

[a] Trp-Na = Trp + 1 eq. $NaHCO_3$. Conditions: $T = 6$ °C, organic phase: DCM, aqueous phase: dd water; [substrate] = 2.0 mM. [a] The distribution D(org/aq) of the substrate (AA) over the two phases is defined as the ratio of the concentration of the substrate over the two phases ($D = [AA]_{org}/[AA]_{aq}$). [b] The operational selectivity (α_{op}) is defined as the ratio of distribution of enantiomers ($\alpha_{op} = D_{D\text{-}AA}/D_{L\text{-}AA}$).

resulting light yellow solution was directly applied in extraction experiments.

The palladium (*R*)-BINAP complex as expected shows distributions and operational selectivities (Table 1, entries 1–4) that correspond well with the palladium (*S*)-BINAP complex (corresponding conditions entry 4: D(org/aq) = 0.5, α_{op} = 2.4).[33] The RP-HPLC data showed that the palladium (*R*)-BINAP complex extracts L-Trp selectively, whereas D-Trp is extracted by the palladium (*S*)-BINAP complex.

Entries 5–8 and 9–12 (Table 1) show the results for the (*S*)-tol-BINAP and the (*S*)-xylyl-BINAP palladium complexes, respectively. In these cases, a preference is shown for the D-Trp. The distributions are essentially constant for all of the palladium complexes examined. For example, $D = 0.5$ for the extraction of Trp-Na (entries 4, 8 and 12). The α_{op} for the palladium (*S*)-tol-BINAP complex is significantly lower (selectivities < 1.8) than for the (*S*)-BINAP complex. In contrast, the (*S*)-xylyl-BINAP palladium complex shows a significantly higher α_{op} (> 3.0). This increase in selectivity is attributed to the increased steric hindrance of the (*S*)-xylyl-BINAP ligand.

Solvent dependence

As noted in our previous publication,[33] the organic solvent employed has a major influence on selectivity, as a consequence of differences in solvation contributions in enantioselective host–guest complexations (Table 2).[34]

The extra methyl groups present in the xylyl moiety of the (*S*)-xylyl-BINAP, make the palladium (*S*)-xylyl-BINAP complex soluble in a wider range of solvents compared to the palladium (*S*)-BINAP complex. However, the complex formed upon extracting Trp-Na into toluene or carbon tetrachloride precipitated (Table 2, entries 5 & 7). The extractions using (*S*)-xylyl-BINAP follow the same trend as observed for (*S*)-BINAP in the solvents tested with the palladium (*S*)-BINAP complex, showing high operational selectivities for dichoromethane and 1,2-dichloroethane (Table 2, entries 2 and 4). It should be emphasized that the use of 1-octanol as a solvent provides a higher α_{op} compared to DCM and 1,2-dichloroethane (Table 2, entry 1), allowing for a non-halogenated solvent as 1-octanol to be applied.

Table 2 Solvent screening

Entry	Solvent	P(org/aq)[a]	D(org/aq)	α_{op}
1	1-Octanol	0.0	0.5	3.3
2	Dichloromethane	0.0	0.5	3.0
3	Chloroform	0.0	0.6	2.4
4	1,2-Dichloroethane	0.0	0.5	3.1
5	Toluene	0.0	0.5*	1.6
6	Chlorobenzene	0.0	0.2	2.8
7	Carbon tetrachloride	0.0	0.5*	1.3
8	1-Butanol	0.6	2.6	1.6
9	*rac*-2-Butanol	0.6	2.9	1.7
10	(*R*)-2-Butanol	0.7	2.7	1.7
11	(*S*)-2-Butanol	0.7	2.3	1.6
12	Octafluoro-pentanol	0.1	1.3	2.2
13	Dodecafluoroheptanol	0.0	1.4	1.8

Conditions: host: $PdCl_2$((*S*)-xylyl-BINAP), Substrate: Trp-Na, [host] = 1.0 mM, [substrate] = 2.0 mM, $T = 6$ °C, aqueous phase: dd water, (*)precipitation/suspension.[a] The physical partition (P) is defined as the distribution (D) of the substrate in absence of a host.

Table 3 Octane/Octanol mixing experiments

Entry	Octane-%	D(org/aq)	α_{op}
1	0	0.5	3.3
2	20	0.4	3.3
3	40	0.3	3.4
4	60	0.3	3.4
5	80	0.0*	—
6	100	0.0*	—

Host: [$PdCl_2$((*S*)-xylyl-BINAP)], Substrate: TRP-Na, [host] = 1.0 mM, [substrate] = 2.0 mM, $T = 6$ °C, aqueous phase: dd water, (*)precipitation/suspension.

The P(org/aq) is 0.6–0.7 for the substrate with the different butanol solvents used as the organic phase (Table 2, entries 8–11) and this can be attributed to the partial miscibility of the butanol solvents and water (*e.g.* 7.7 g 1-butanol per 100 mL water). As noted, physical partition of the substrate reduces the achievable α_{op}. Fluorinated alcohols (Table 2, entries 12 and 13) provide little to no physical partition, but nevertheless show lower α_{op} than 1-octanol and the halogenated solvents. This lowering of the α_{op} is probably due to increased polarity of perfluorinated alcohols compared to alkyl alcohols, which has been attributed to strong hydrogen bonding.[35]

The relation between organic solvent polarity and α_{op} was examined by varying the amount of octane mixed with 1-octanol. As the percentage of octane is increased (Table 3, entries 1 to 4), the distribution decreases compared to neat 1-octanol. The decreased polarity of the organic solvent disfavors formation of the complex. However, the α_{op} increases slightly to 3.4. At 80% octane and higher, immediate precipitation of the host occurred (Table 3, entries 5 and 6).

Substituent effects of the substrate

Phenylalanine analogues. The substrate scope was examined using a series of Phe analogues and $PdCl_2$((*S*)-BINAP) as a host in a number of solvents. The relation between the electronic effects of the substituents in the substrate Phe and α_{op}, were investigated

Table 4 Relationship between host and substrate

Entry	Substrate	P(org/aq)	D(org/aq)	α_{op}
1	4Cl-Phe[a]	0.0	0.7	3.3
2	4F-Phe	0.0	0.5	2.9
3	Phe	0.0	0.4	2.5
4	4MeO-Phe	0.0	0.5	2.4

Conditions: Host: [$PdCl_2$((*S*)-BINAP)], [host] = 1.0 mM, [substrate] = 2.0 mM, organic phase = DCM, T = 6 °C, 1 eq. $NaHCO_3$.[a] 4X-Phe represents an underivatized phenylalanine with the X substituent at the *para*-position.

Table 6 Phenylalanine analogues in 1-octanol

Entry	Substrate	P(org/aq)	D(org/aq)	α_{op}
1	4CF_3-Phe	0.5	1.9	1.2
2	4Br-Phe	0.3	6.0	1.7
3	4Cl-Phe	0.1	0.7	1.1
4	4F-Phe	0.0	0.5	2.1
5	Phe	0.0	0.4	1.9
6	4MeO-Phe	0.0	0.5	1.8

Conditions: Host = $PdCl_2$((*S*)-*xylyl*-BINAP), [host] = 0.25 mM, [substrate] = 2.0 mM, org = 1-octanol, aq = dd., T = 6 °C, 1 eq. $NaHCO_3$.

using Phe derivatives substituted with electron donating and electron withdrawing groups at the *para*-position. All of the Phe analogues have a distribution between 0.4 and 0.7 (Table 4). The α_{op} however, shows an increase with increasing electron withdrawing groups at the *para*-position. The α_{op} increases from 2.4 for the electron-donating methoxy group (entry 4) to 3.3 for the electron-withdrawing chloride group (entry 1).

With the $PdCl_2$((*S*)-xylyl-BINAP) complex as the host, a wider substrate scope of Phe analogues was extracted (Table 5) in a number of halogenated organic solvents. As with tryptophan, the palladium complex with the (*S*)-xylyl-BINAP ligand shows higher α_{op} than with the (*S*)-BINAP ligand (Table 4). For example, in the case of Phe, the α_{op} is 2.5 in the case of (*S*)-BINAP (Table 4, entry 3) whereas it is increased to 4.4 with (*S*)-xylyl-BINAP (Table 5, entry 6).

As with (*S*)-BINAP, a relationship is observed between the electron-withdrawing or donating property of the substituent on the *para* position of the phenyl ring of the Phe analogue and the α_{op}. The Phe analogues bearing an electron withdrawing group show selectivities above 5.7 in DCM (entries 1–5), whereas Phe and 4MeO-Phe show α_{op} = 4.4 (entries 6, 7). The selectivity of 4.4 observed for Phe is the highest selectivity observed to date for Phe using chiral metal complexes as hosts. The α_{op} of the other analogues represent the highest selectivities reported to date and the α_{op} of 7.0 for 4Br-Phe allows full separation of both enantiomers in a 6 stage CCS cascade.

A correlation between the polarity index *P'*, which is a measure of the polarity of the solute–solvent interactions,[36] and α_{op} is observed. Dichloromethane has the lowest polarity of 3.4, while chloroform and 1,2-dichloroethane have a polarity index of 3.7 and 4.4, respectively. The lower polarity of dichloromethane appears to benefit the selectivity of the extraction, as the tested Phe analogues, all show the same trend of increasing α_{op} with decreasing polarity.

When 1-octanol is used as the organic phase (Table 6) the physical partitioning of the CF_3-, Br and Cl-Phe analogues (entries 1–3) should be noted. This physical partition is not observed using halogenated solvents (Table 5). The observed physical partition with 1-octanol as an organic solvent also has a dramatic effect on the distribution, which is up to 6.0 for 4Br-Phe (entry 2). Phe shows a distribution of 0.4 (entry 5) which is comparable to the distributions observed in halogenated solvents (Table 5, entries 6, 13, 20). The observed α_{op} in 1-octanol does not correspond to its polarity index of 3.2, which is presumably due to additional interactions of 1-octanol with the substrate, as observed in entries 1–3.

Table 5 The ELLE of Phe analogues with $PdCl_2$((*S*)-xylyl-BINAP) and a number of organic solvents

Entry	Substrate	Solvent	P(org/aq)	D(org/aq)	α_{op}
1	4NO_2-Phe	DCM	0.0	0.8	6.7
2	4CF_3-Phe	DCM	0.0	1.9	6.3
3	4Br-Phe	DCM	0.0	1.7	7.0
4	4Cl-Phe	DCM	0.0	0.9	6.4
5	4F-Phe	DCM	0.0	0.7	5.7
6	Phe	DCM	0.0	0.6	4.4
7	4MeO-Phe	DCM	0.0	0.7	4.4
8	4NO_2-Phe	1,2-dce	0.0	0.7	5.8
9	4CF_3-Phe	1,2-dce	0.0	1.4	5.3
10	4Br-Phe	1,2-dce	0.0	1.3	6.0
11	4Cl-Phe	1,2-dce	0.0	0.8	6.0
12	4F-Phe	1,2-dce	0.0	0.5	5.2
13	Phe	1,2-dce	0.0	0.5	4.3
14	4MeO-Phe	1,2-dce	0.0	0.6	4.2
15	4NO_2-Phe	$CHCl_3$	0.0	0.9	4.2
16	4CF_3-Phe	$CHCl_3$	0.0	2.5	5.0
17	4Br-Phe	$CHCl_3$	0.0	2.3	4.9
18	4Cl-Phe	$CHCl_3$	0.0	0.9	4.3
19	4F-Phe	$CHCl_3$	0.0	0.8	4.3
20	Phe	$CHCl_3$	0.0	0.7	3.3
21	4MeO-Phe	$CHCl_3$	0.0	0.8	3.2

Conditions: host = $PdCl_2$((*S*)-xylyl-BINAP), [host] = 1.0 mM, [substrate] = 2.0 mM, T = 6 °C, 1 eq. $NaHCO_3$

N-Acetyl protected amino acids

The distribution of acetyl protected amino acids is shown in Table 7. The free carboxylate group is necessary for the binding to the palladium complex. The distribution changes from 0.5 for unprotected Trp (Table 4.1, entry 7) to 1.1 for the *N*-acetyl protected Trp. The pK_a of the dissocation constant of the NH_3^+ group of Trp is 9.39,[37] whereas the pK_a of *N*-acetyl protected amino acids is around 3.6.[38] As a result, the concentration of the substrate in its anionic form will be higher in the case of *N*-Ac-Trp at the pH conditions of the experiments.

Comparison of the α_{op} of the protected Trp with the unprotected Trp are compared, and a significant decrease is observed. The α_{op} is 1.6 for *N*-Ac-Trp-Na (entry 3) compared to α_{op} = 2.4 for Trp-Na.[33] The free amine group of Trp is supposed to interact with the palladium[39] to induce operational selectivity. There is a clear relationship between the host/substrate stoichiometry and the α_{op}, with α_{op} increasing with higher concentrations of host relative to the substrate. This indicates that a different extraction mechanism is involved. Typically, host/substrate stoichiometry dependent α_{op} behaviour is indicative for a homogeneous mechanism rather than

Table 7 ELLE of *N*-Ac protected amino acids

Entry	Substrate	[host]/mM	D(org/aq)	α_{op}
1	*N*-Ac-Trp	5.0	1.1	1.5
2	*N*-Ac-Trp	1.0	0.5	1.1
3	*N*-Ac-Trp-Na	5.0	2.3	1.6
4	*N*-Ac-Trp-Na	1.0	0.5	1.0
5	*N*-Ac-Pge	5.0	1.4	1.2
6	*N*-Ac-Pge	1.0	0.5	1.0
7	*N*-Ac-Pge-Na	5.0	1.8	1.3
8	*N*-Ac-Pge-Na	1.0	0.5	1.1
9	*N*-Ac-Phe	5.0	1.6	1.2
10	*N*-Ac-Phe	1.0	0.5	1.1
11	*N*-Ac-Phe-Na	5.0	3.0	1.3
12	*N*-Ac-Phe-Na	1.0	0.5	1.0

Conditions: host = $PdCl_2$((*S*)-BINAP), [substrate] = 2.0 mM, T = 6 °C, 1 eq. $NaHCO_3$.

an interface mechanism.[20] This implies that the *N*-acetyl protected substrate will diffuse into the organic phase prior to complexation.

Counterion, temperature, concentration and kinetic studies

Counterion effect. To evaluate the effect of the counterions of the palladium host, *in situ* experiments with palladium salts and three halogen anions, nitrate and acetate as counterions were performed. Data from single extraction experiments are summarized in Table 8. A strong relationship between the nature of the halide anion and the distribution is revealed. The distribution drops from 0.8 with the chloride (entry 1) to 0.1 with the iodide anion (entry 3). This effect is attributed to the lipophilicity and hence the increased polarizability of the halide anions with increasing atomic number. The lipophilicity of iodide and its subsequent low aqueous solubility compared to chloride shifts the equilibrium of the complex formation of the substrate (Trp) with the palladium in favour of the complex. This is a recurrent phenomenon in the field of phase-transfer catalysis.[40] The increased α_{op} of the host with the bromide anion (entry 2) could be an indication for an improved interaction of the substrate with the host. Unfortunately, the distribution of the iodide anion complex (entry 3) was too low to determine the α_{op}.

When nitrate is used as a counterion (entry 4), distributions and selectivities are comparable to those employing chloride (entry 1) are observed. In the case of an acetate counterion (entry 5), a comparable distribution to the chloride counterion is achieved, but with a much lower α_{op}.

Table 8 The effect of the halogen anion of the host

Entry	Metal precursor	D(org/aq)	α_{op}
1	$PdCl_2$	0.8	2.2
2	$PdBr_2$	0.4	2.7
3	PdI_2	0.1	—
4	$Pd(NO_3)_2$	0.7	2.4
5	$Pd(OAc)_2$	0.9	1.3

Conditions: ligand: (*S*)-BINAP, substrate = Trp-Na, [metal precursor] = 1.0 mM, [ligand] = 1.1 mM, [substrate] = 2.0 mM, T = 6 °C, org = DCM, aq = dd.

Temperature Dependence studies

The distribution and α_{op} of the ELLE of Trp using $PdCl_2$((*S*)-BINAP) as a host were determined in the temperature interval from T = 6 °C to 60 °C. 1-Octanol was chosen as the organic phase, due to its high boiling point (195 °C).

Below T = 30 °C, the distribution increases slightly from 0.5 to 0.6. Above T = 40 °C, the distribution increases to a value above 1.0 (Fig. 5a). A distribution above 1.0 at a host concentration of 1.0 mM indicates that the concentration of substrate in the organic layer exceeds the concentration of host. This overloading[41] of substrate with respect to the host most probably involves the complexation of a second amino acid on the palladium.

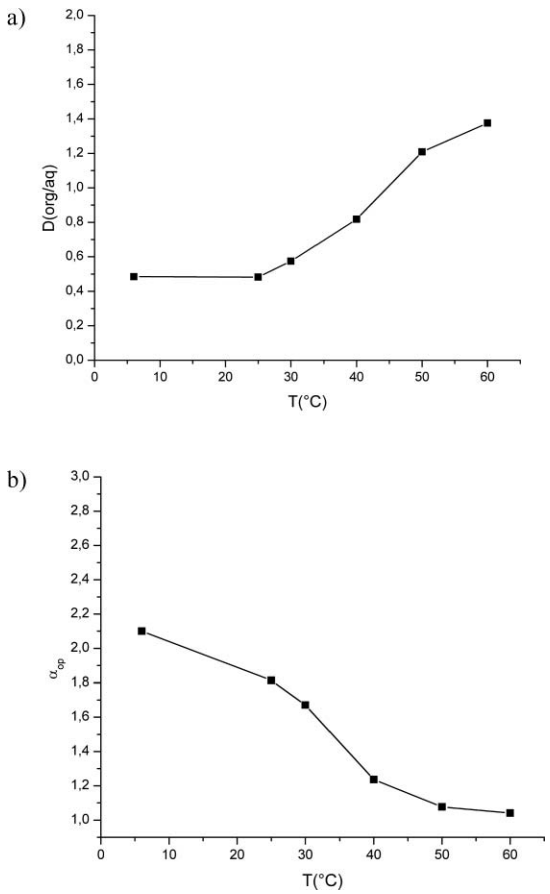

Fig. 5 The relation between temperature and the distribution (a) and the α_{op} (b) of the ELLE of Trp. Conditions: $PdCl_2$((*S*)-BINAP) (1.0 mM), Trp-Na (2.0 mM), n-octanol, dd. water. Lines are a guide to the eye.

The α_{op} decreases with increasing temperature. Over the temperature range 6–40 °C, the distribution remains below 1.0 and the α_{op} decreases with increasing temperature (Fig. 5b).[42] When the distribution is above 1.0, the α_{op} decreases below 1.2 and the host-substrate interaction becomes essentially nonselective. Optimal selectivity is achieved at lower temperatures. However, below T = 6 °C, extraction becomes too difficult due to an increase in viscosity of the solution and the decrease of host and substrate solubility. Therefore in this case, T = 6 °C is considered to be the optimal temperature for enantioselective extraction.

Table 9 The ELLE of Trp at various concentrations

Entry	[host]	[substrate]	D(org/aq)	α_{op}
1	2.0	4.0	0.42	2.3
2	4.0	8.0	0.42	2.4
3	6.0	12.0	0.76	2.2
4	8.0	16.0	0.71	2.4
5	10.0	20.0	0.76	2.3

Conditions: $PdCl_2$((*S*)-BINAP), substrate = Trp-Na, organic solvent = DCM, aqueous phase = dd. Water, $T = 6$ °C.

Concentration dependence and kinetics

The concentration of both the host and the substrate can be increased compared to the standard ELLE experiments performed in this study. The behaviour of the extraction system at increased concentrations is of special importance in application of ELLE to a CCS cascade.

The concentration dependence on distribution and α_{op} are shown in Table 9. The increase of the distribution with increasing concentration (from $D = 0.42$ for $c_{host} = 2.0$ mM to $D = 0.76$ for $c_{host} = 10.0$ mM) is due to the increase in pH, which is a result of the increase of concentration of sodium-Trp. As expected, the α_{op} remains constant over the concentration range examined.

The time of equilibration was determined using a reaction vessel as depicted in Fig. 6. Stirring was done at rotation speeds of 800, 900 and 1,000 rpm. This resulted in fully disperse conditions and represents the conditions in a CCS, with equilibration being achieved within 2 min. This time interval is well within the hold-up time in a single stage of a CCS cascade and hence the extraction system is fast enough for application in a CCS cascade.

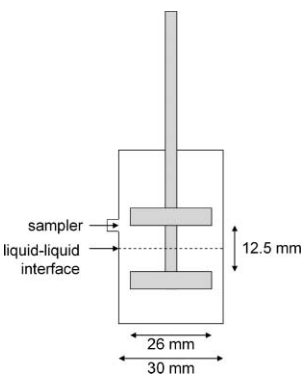

Fig. 6 Reaction vessel scheme. Conditions: host: [$PdCl_2$((*S*)-BINAP)], substrate = D-Trp-Na, [host] = 0.1 mM, [substrate] = 0.2 mM, org = DCM, aq = dd, T = rT, V(org) = 10 mL, V(aq) = 10 mL.

^{31}P-NMR Spectroscopy

^{31}P-NMR spectroscopic studies were carried out using $PdCl_2$((*S*)-BINAP) in $CDCl_3$ at $c = 5.0$ mM and AA-Na at $c = 50.0$ mM. The ^{31}P-NMR spectra of the $PdCl_2$((*S*)-BINAP) complex upon titration of the enantiomers of Trp has been reported by us previously.[33] Here a temperature dependence ^{31}P-NMR study is presented (Fig. 7). (*S*)-BINAP acts as an internal standard. At higher temperatures ($T = 40$ °C) the two complexes show distinct absorptions: the PdCl((*S*)-BINAP)-D-Trp complex, which is the preferred diastereomer formed in ELLE, shows a single, defined

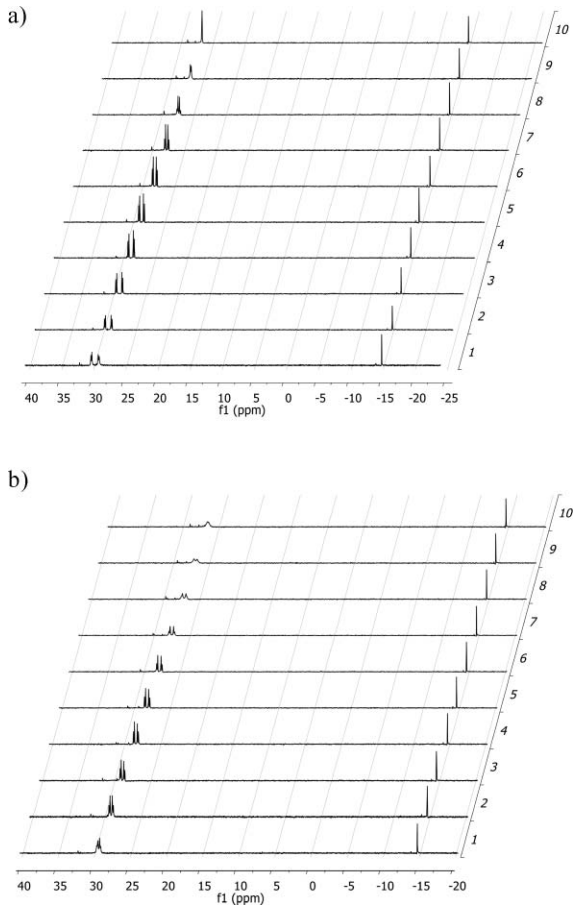

Fig. 7 Temperature dependent studies on the PdCl((*S*)-BINAP)-D-Trp (a) and PdCl((*S*)-BINAP)-L-Trp (b) complex. Spectra 1–10 represent T = –50 °C to +40 °C at 10 °C intervals.

absorption (Fig. 7a, spectrum 10), where the PdCl((*S*)-BINAP)-L-Trp shows a broad ill-defined absorption (Fig. 7b, spectrum 10).

The temperature was decreased with 10 °C intervals in the case of PdCl((*S*)-BINAP)-D-Trp (Fig. 7a), the singlet absorption splits up into an AB-system with the two absorptions at 29.50 and 28.55 ppm and a coupling constant of $J = 31.4$ Hz at $T = -40$ °C (spectrum 2).

Similar results are obtained with the PdCl((*S*)-BINAP)-L-Trp complex. The ill-defined absorption splits up into an AB-system with the two absorptions at a shift of 29.25 and 28.78 ppm and a coupling constant of $J = 31.2$ Hz. The coupling constant in both diastereomeric complexes is almost the same, whereas the difference in chemical shift of the complexes is $\delta\delta\delta = 0.48$ ppm. The larger change in the chemical shift is observed with the PdCl((*S*)-BINAP)-D-Trp complex. This is another indication of the more stable host-substrate complex formed by the palladium host and the D-Trp enantiomer. The difference in chemical shift observed for the AB-systems of both diastereomeric complexes could imply a method for direct determination of the diastereomeric excess of the host-substrate complexes.[43;44] The attempt to direct diastereomer determination by ^{31}P-NMR is depicted in Fig. 8.

Unfortunately, no accurate analysis could be made, since the absorptions overlap, even at lower temperature (Fig. 8). Other amino acids (Phe, Pro, Val, Asp) were tested, but did not provide well resolved ^{31}P-NMR absorptions. On the contrary, in the case of

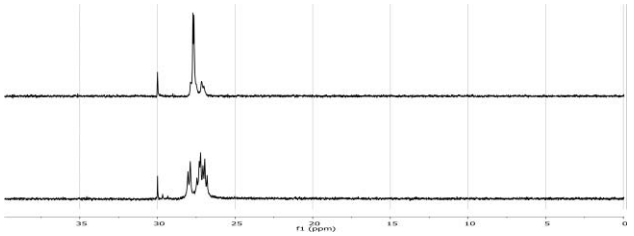

Fig. 8 ^{31}P-NMR spectra of the organic phase of the ELLE of DL-Trp-Na, taken at $T = -40$ °C (bottom) and +20 °C (top). Conditions ELLE: host = [$PdCl_2$((*S*)-BINAP)], [host] = 10.0 mM, [substrate] = 20.0 mM, $T = 6$ °C.

Cys, excellent separated absorptions were observed even at room temperature, presumably as a result of the coordination of the thiol functionality of Cys to the palladium metal centre.[45] Fig. 9 shows the ^{31}P-NMR spectrum of the $PdCl_2$((*S*)-BINAP) complex upon titration of Cys. Two sets of two doublets can be seen, the first set of doublets is at $\delta = 32.1$ and 16.9 ppm with $J = 35.3$ Hz. The second set is at $\delta = 31.1$ and 17.6 ppm with $J = 32.4$ Hz. The two sets can be identified as two AB-systems, which represent the two diastereomers of D-Cys and L-Cys bound to the host. The ratio by NMR integration is 1.4, which represents an ee of 20% for D-Cys in the organic phase. This corresponds to $\alpha_{op} = 2.2$ if $D = 1.0$.

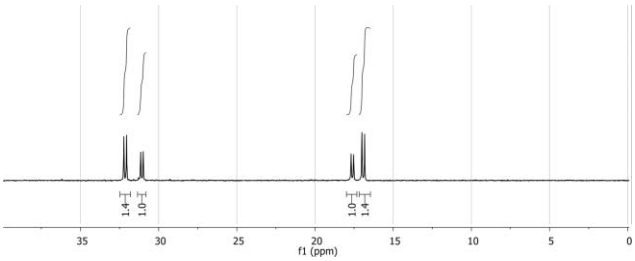

Fig. 9 ^{31}P-NMR spectra of the organic phase of the ELLE of DL-Cys-Na, taken at $T = -40$ °C. Conditions ELLE: host = $PdCl_2$((*S*)-BINAP), [host] = 10.0 mM, [substrate] = 20.0 mM, $T = 6$ °C.

UV-Vis and CD Spectroscopy

UV-Vis and CD spectroscopy were employed to study the binding of Trp to $PdCl_2$((*S*)-BINAP) by titration of the Trp enantiomers. The titration involved the increase of concentration of a Trp enantiomer in the aqueous phase in an extraction experiment.

The UV-Vis spectra of the titration of D-Trp to the $PdCl_2$((*S*)-BINAP) complex shows an isosbestic point at 328 nm and a decrease in absorption above 328 nm (Fig. 10a). The differential spectra (Fig. 10b) reveal two minima in absorption, at $\lambda = 335$ nm and $\lambda = 365$ nm. A difference in the maximum is observed at $c =$ 10.0 mM for both substrate enantiomers: D-Trp shows the largest change in absorption.

The CD spectra of $PdCl_2$((*S*)-BINAP) upon titration of D-Trp (Fig. 11a) show a bathochromic shift from $\lambda = 363$ nm to $\lambda =$ 375 nm. A hypsochromic shift is observed for the maximum at $\lambda = 345$ nm, which shifts to $\lambda = 343$ nm upon titation of D-Trp. A bathochromic shift is observed at $\lambda = 325$ nm, which shifts to $\lambda =$ 329 nm upon titration of D-Trp.

The CD differential spectra reveal corresponding ellipticities for the titration of both Trp enantiomers (Fig. 11b). The higher ellipticity at $\lambda = 340$ nm for D-Trp can be explained by the higher

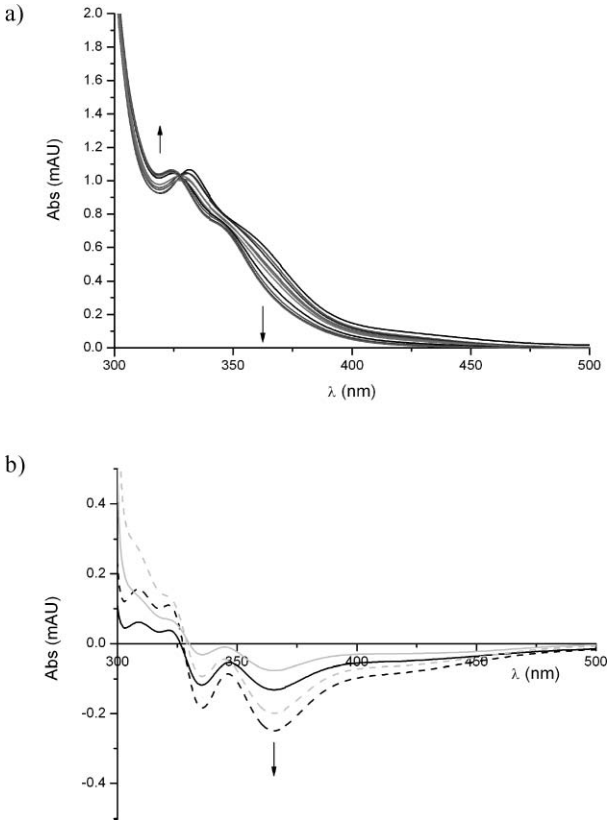

Fig. 10 UV-Vis spectra of $PdCl_2$((*S*)-BINAP) upon titration of D-Trp (0.0–10.0 mM) (left) and UV-Vis differential spectra (right) of D-Trp (black) and L-Trp (grey) at 1.0 (solid) and 10.0 mM (dashed).

affinity of the $PdCl_2$((*S*)-BINAP) for the D-Trp enantiomer. At higher concentration ($c = 10.0$ mM), only a minor difference at $\lambda = 417$ nm (Fig. 11b) is observed, whereas the difference in the absorption in the UV-Vis spectra is observed over the entire measured wavelength interval.

These results suggest the binding of both the Trp enantiomers to the palladium complex is similar, resulting in a similar type of geometry of the palladium complexes. The slight difference in ellipticity at $\lambda = 417$ nm is the only indication of the observed preference of the D-Trp enantiomer over the L-Trp enantiomer observed in the ELLE experiments *vide supra.*

FTIR Spectroscopy. FTIR spectra were taken for the $PdCl_2$((*S*)-BINAP) complex and the PdCl((*S*)-BINAP)-D-Trp complex (Fig. 12).

The strong absorption band at 1654 cm^{-1} can be assigned to the carboxylate anion[46] complexed to the palladium. The absorption band at 3309 cm^{-1} can be assigned to the stretching vibrations of the primary amine group coordinated to the palladium metal center.[47]

To confirm the coordination of the amine to the palladium, a comparison between the tryptophan palladium complex and the tryptophan sodium complex (H_2N-CHR-CO_2Na) was made by FTIR spectrscopy. The FTIR spectra of the complexes are depicted in Fig. 13. The stretching band of the primary amine of the sodium salt of Trp appears at 3382 cm^{-1}, whereas the corresponding band of the palladium complex appears at 3309 cm^{-1} as mentioned before. This difference in wavenumber is an additional

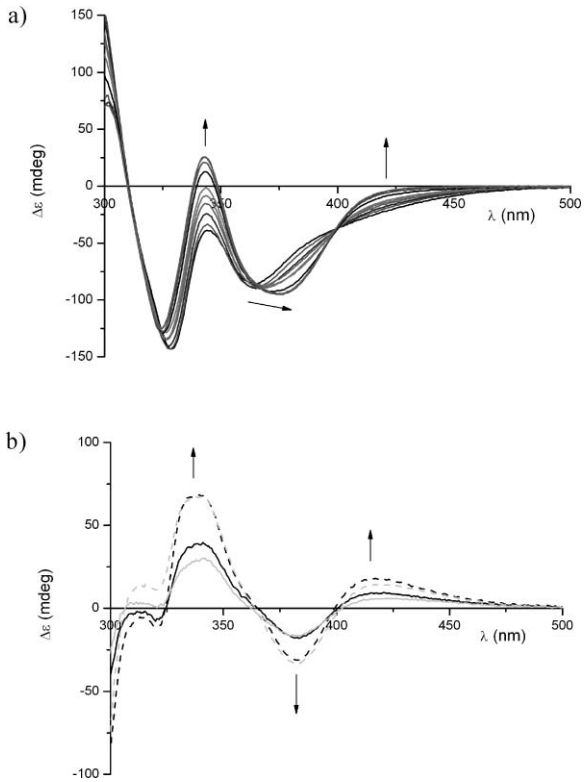

Fig. 11 CD spectra of $PdCl_2$((*S*)-BINAP) upon titration of D-Trp (0.0–10.0 mM) (a) and CD differential spectra (b) of D-Trp (black) and L-Trp (grey) at 1.0 mM (solid) and 10.0 mM (dashed).

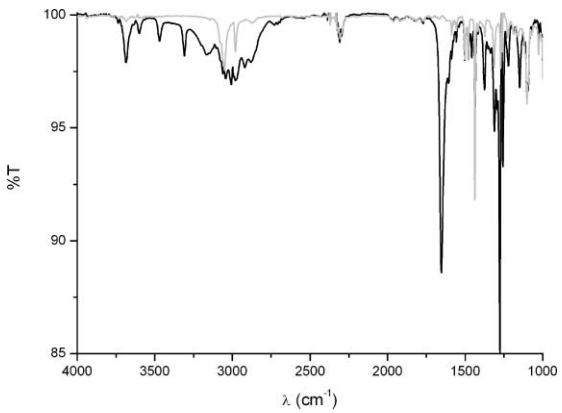

Fig. 12 FTIR spectra of $PdCl_2$((*S*)-BINAP) (grey) and PdCl((*S*)-BINAP)(D-Trp) (black).

indication for the primary amine coordinating to the palladium metal center.[39,48]

FT-FIR and Raman Spectroscopy. For $PdCl_2$((*S*)-BINAP), Pd–Cl stretching bands were found at wavenumbers corresponding to those in the literature: 306 and 292 cm^{-1} (Fig. 14).[49] The spectra of both $PdCl_2$((*S*)-BINAP) and PdCl((*S*)-BINAP)-D-Trp were normalized at 504 cm^{-1}. The aforementioned Pd–Cl bands decrease in intensity in the spectrum of PdCl((*S*)-BINAP)-D-Trp and shift to 314 and 302 cm^{-1}.

The Raman spectrum of the $PdCl_2$((*S*)-BINAP) (Fig. 15a) shows absorptions at 302 and 290 cm^{-1} which can be assigned to the Pd–Cl stretching band.[50] The band at 302 cm^{-1} is not present

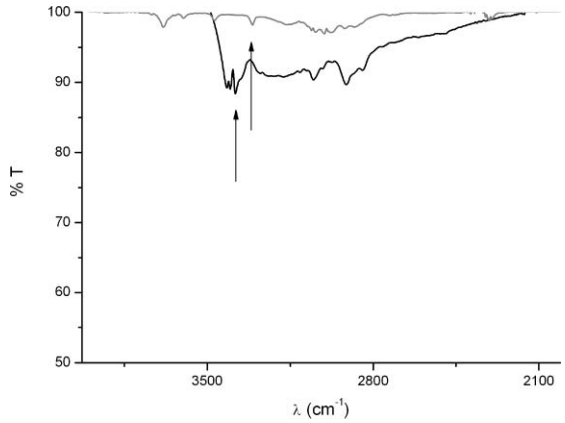

Fig. 13 FTIR spectra of PdCl((*S*)-BINAP)(D-Trp) (grey) and Trp-Na (black). Arrows indicate absorption bands assigned to the stretching vibrations of the primary amine.

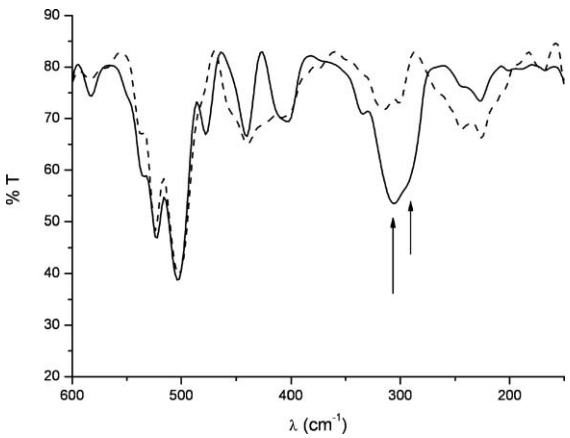

Fig. 14 FT-FIR spectra of $PdCl_2$((*S*)-BINAP) (black) and PdCl((*S*)-BINAP)-D-Trp (dashed).

in the spectrum of the PdCl((*S*)-BINAP)-D-Trp complex, whereas the band at 290 cm^{-1} has decreased in intensity and shifted to 288 cm^{-1} (Fig. 15b).

Structure of the complex

As is shown in our previous publication, the amino acid substrate binds to the palladium complex in a 1 : 1 ratio at neutral pH conditions, proven by extraction experiments, ESI-MS, NMR spectroscopy and the calculation of association constants.[33]

The results of the Far IR and Raman spectroscopy suggest the dissociation of at least one Pd–Cl bond. The other Pd–Cl bond is supposed to be either noncoordinating (indicated by the loss of absorption in the Raman spectrum), or less coordinating (indicated by the decrease in intensity in the FT-FIR spectrum). The FT-IR spectrum shows a shift in the bands of the amine. This could indicate a coordination to the palladium.

All this evidence points to a coordination of the amino acid in a bidentate fashion to the palladium complex as proposed in Fig. 16. The bidentate complexation is a valid explanation for the observed high operational selectivities using metal complexes.[51] The three point interaction rule (TPI)[52] is commonly used in ELLE to explain the mechanism behind selective binding.[31,32] The first two interactions are attracting interaction and are provided by the

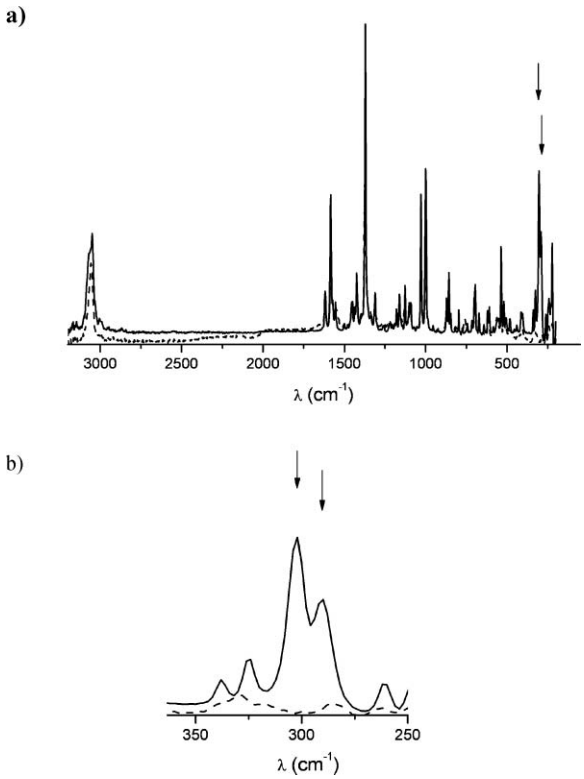

Fig. 15 Raman spectra of [$PdCl_2$((*S*)-BINAP)] (black) and [PdCl((*S*)-BINAP)D-Trp] (dashed) (a) and inset at 250–350 cm^{-1} (b).

bidentate complexation of the amino acid. The third interaction is either a repulsion interaction (*e.g.* steric), or an attracting interaction (*e.g.* π–π stacking) between the side-group of the amino acid and the (*S*)-BINAP ligand. When halogenated solvents are used for the extraction of Phe analogues, a relationship is observed between the electronic properties of the aromatic ring of the Phe analogues and the α_{op}. The increased α_{op} in the case of electron deficient rings of the Phe analogues suggest an attracting π–π interaction between the substrate and the phenyl rings of the ligand of the palladium complex. This is supported by the increased α_{op} as the electron density on the phenyl rings of the ligand is increased ((*S*)-BINAP *vs.* (*S*)-xylyl-BINAP).

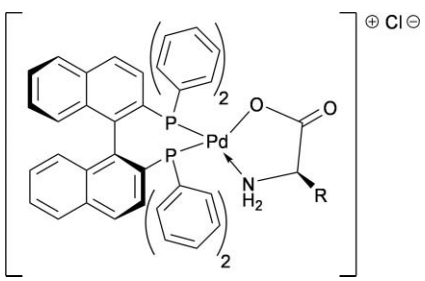

Fig. 16 Proposed structure of the [PdCl((*S*)-BINAP)D-Trp] complex.

Conclusions and outlook

The host $PdCl_2$((*S*)-xylyl-BINAP) shows unprecedented high selectivities for a range of Phe analogues. The system's α_{op} can be optimized by changing the ligand, the organic solvent, the temperature and the nature of the substrate. The combined spectroscopic evidence suggests a bidentate complexation of the substrate to the host and a three-point interaction causing the enantioselectivity. For future application in a CCS cascade, the system meets all the required properties such as a high selectivity (which dramatically limits the number of required stages), reversibility, versatility, easy distribution control and sufficient concentration and kinetic properties.

Acknowledgements

We thank Dr W.R. Browne for useful discussions. This research was financially supported by the Netherlands Organisation for Scientific Research (NWO) through the Separation Technology program in cooperation with DSM and Schering-Plough.

Notes and references

1 M. Breuer, K. Ditrich, T. Habicher, B. Hauer, M. Kesseler, R. Sturmer and T. Zelinski, *Angew. Chem., Int. Ed.*, 2004, **43**, 788.
2 J. S. Carey, D. Laffan, C. Thomson and M. T. Williams, *Org. Biomol. Chem.*, 2006, **4**, 2337.
3 W. Liu, ed. D. J. Ager, CRC-Taylor & Francis, Boca Raton, 2 edn, 2006, pp. 75-95.
4 R. N. Patel, in *Stereoselective Biocatalysis*, Marcel Dekker, New York, 2000.
5 O. Pamies and J. E. Backvall, *Chem. Rev.*, 2003, **103**, 3247.
6 Y. Fujima, M. Ikunaka, T. Inoue and J. Matsumoto, *Org. Process Res. Dev.*, 2006, **10**, 905.
7 A. N. Collins, G. N. Sheldrake and J. Crosby, in *Chirality in Industry II*, New York, Wiley and Sons, 1997, pp. 411.
8 S. Houlton, *Manuf.Chem.*, 2001, **72**, 16.
9 W. L. Noorduin, T. Izumi, A. Millemaggi, M. Leeman, H. Meekes, W. J. P. Van Enckevort, R. M. Kellogg, B. Kaptein, E. Vlieg and D. G. Blackmond, *J. Am. Chem. Soc.*, 2008, **130**, 1158.
10 E. M. van der Ent, T. P. H. Thielen, M. A. C. Stuart, A. von der Padt and J. T. F. Keurentjes, *Ind. Eng. Chem. Res.*, 2001, **40**, 6021.
11 D. Kozma and E. Fogassy, *Chirality*, 2001, **13**, 428.
12 S. Keszei, B. Simandi, E. Szekely, E. Fogassy, J. Sawinsky and S. Kemeny, *Tetrahedron: Asymmetry*, 1999, **10**, 1275.
13 B. Simandi, S. Keszei, E. Fogassy, S. Kemeny and J. Sawinsky, *J. Supercrit. Fluids*, 1998, **13**, 331.
14 B. Simandi, S. Keszei, E. Fogassy and J. Sawinsky, *J. Org. Chem.*, 1997, **62**, 4390.
15 M. Steensma, in *Chiral Separation of amino-alcohols and amines by fractional reactive extraction*, Ph.D. thesis, University of Twente, The Netherlands, 2005.
16 E. Eliel, S. Wilen and L. Mander, in *Stereochemistry of organic compounds*, Wiley, New York, N.Y., 1994, ch. Chapter 7-7, pp. 416-424.
17 G. J. Quallich, *Chirality*, 2005, **17**, S120.
18 L. A. Robbins, in *Handbook of separation technology for chemical engineers*, ed. P. A. Schweitzer, New York, McGraw-Hill, 3 edn, 1997, pp. 1419-1447.
19 M. Steensma, N. J. M. Kuipers, A. B. De Haan and G. Kwant, *Chem.Eng.Proc.*, 2007, **46**, 996.
20 M. Steensma, N. J. M. Kuipers, A. B. De Haan and G. Kwant, *Chirality*, 2006, **18**, 314.
21 A. Maximini, H. Chmiel, H. Holdik and N. W. Maier, *J. Membr. Sci.*, 2006, **276**, 221.
22 E. Gavioli, N. M. Maier, C. Minguillon and W. Lindner, *Anal. Chem.*, 2004, **76**, 5837.
23 A. J. Hallett, G. J. Kwant and J. G. de Vries, *Chem. Eur. J.*, 2008, 2111.
24 B. Schuur, J. Floure, A. J. Hallett, J. G. M. Winkelman, J. G. de Vries and H. J. Heeres, *Org. Process Res. Dev.*, 2008, **12**, 950.
25 B. Schuur, W. J. Jansma, J. G. M. Winkelman and H. J. Heeres, *Chem.Eng.Proc.*, 2008, **47**, 1484.
26 B. Schuur, A. J. Hallett, H. J. Heeres and J. G. de Vries, *Org. Process Res. Dev.*, 2009, **13**, 911.

27 M. Steensma, N. J. M. Kuipers, A. B. De Haan and G. Kwant, *Chem. Eng. Sci.*, 2007, **62**, 1395.
28 S. S. Peacock, D. M. Walba, F. C. A. Gaeta, R. C. Helgeson and D. J. Cram, *J. Am. Chem. Soc.*, 1980, **102**, 2043.
29 D. S. Lingenfelter, R. C. Helgeson and D. J. Cram, *J. Org. Chem.*, 1981, **46**, 393.
30 A. Galan, D. Andreu, A. Echavarren, P. Prados and J. De Mendoza, *J. Am. Chem. Soc.*, 1992, **114**, 1511.
31 H. Tsukube, S. Shinoda, J. Uenishi, T. Kanatani, H. Itoh, M. Shiode, T. Iwachido and O. Yonemitsu, *Inorg. Chem.*, 1998, **37**, 1585.
32 T. Takeuchi, R. Horikawa and T. Tanimura, *Anal. Chem.*, 1984, **56**, 1152.
33 B. J. V. Verkuijl, A. J. Minnaard, J. G. de Vries and B. L. Feringa, *J. Org. Chem.*, 2009, **74**, 6526.
34 K. A. Schug and W. Lindner, *Chem. Rev.*, 2005, **105**, 67.
35 M. Koichi, in *Green Reaction Media in Organic Synthesis*, Wiley-Blackwell, New York, 2005.
36 L. R. Snyder, *J. Chromatogr., A*, 1974, **92**, 223.
37 D. R. Lide, in *Handbook of Chemistry and Physics*, CTC Press, 75 edn, 1994, ch. Chapter 7, pp. 1-2.
38 E. J. King and G. W. King, *J. Am. Chem. Soc.*, 1956, **78**, 1089.
39 A. D. Burrows, D. M. P. Mingos, A. J. P. White and D. J. Williams, *J. Chem. Soc., Dalton Trans.*, 1996, 149.
40 M. Makosza and A. Chesnokov, *Tetrahedron*, 2008, **64**, 5925.
41 J. A. Tamada and C. J. King, *Ind. Eng. Chem. Res.*, 1990, **29**, 1327.
42 B. Tan, G. S. Luo and H. D. Wang, *Tetrahedron: Asymmetry*, 2006, **17**, 883.
43 Y. Perez-Fuertes, A. M. Kelly, A. L. Johnson, S. Arimori, S. D. Bull and T. D. James, *Org. Lett.*, 2006, **8**, 609.
44 J. Bravo, C. Cativiela, J. E. Chaves, R. Navarro and E. P. Urriolabeitia, *Inorg. Chem.*, 2003, **42**, 1006.
45 W. Henderson, L. J. McCaffrey and B. K. Nicholson, *J. Chem. Soc., Dalton Trans.*, 2000, 2753.
46 M. Hesse, H. Meier and B. Zeeh, in *Spektroskopische Methoden in der organische Chemie*, Georg Thieme Verlag, Stuttgart, New York, 1984.
47 H. Dialer, P. Mayer, K. Polborn and W. Beck, *Eur. J. Inorg. Chem.*, 2001, 1051.
48 A. Bohm and D. Seebach, *Helv. Chim. Acta*, 2000, **83**, 3262.
49 M. Cataldo, E. Nieddu, R. Gavagnin, F. Pinna and G. Strukul, *J. Mol. Catal. A: Chem.*, 1999, **142**, 305.
50 S. M. O. Quintal, H. I. S. Nogueira, V. Felix and M. G. B. Drew, *New J. Chem.*, 2000, **24**, 511.
51 T. B. Reeve, J. P. Cros, C. Gennari, U. Piarulli and J. G. de Vries, *Angew. Chem., Int. Ed.*, 2006, **45**, 2449.
52 V. A. Davankov, *Chirality*, 1997, **9**, 99.

